GEOPHYSICAL RESEARCH LETTERS, VOL. 28, NO. 5, PAGES 903-906, MARCH 1, 2001

Modeling Jupiter's synchrotron radiation

Steven M. Levin, Scott J. Bolton, Samuel L. Gulkis, and Michael J. Klein

Jet Propulsion Laboratory, Caltech Pasadena, California

Bidushi Bhattacharya and Richard M. Thorne

Department of Atmospheric Sciences, UCLA

Abstract. We have constructed a computer model to simulate synchrotron emission from relativistic electrons trapped in Jupiter's magnetic field. The computer program generates the four Stokes parameters of the synchrotron emission for assumed electron distributions and magnetic field models. The resulting two dimensional Stokes parameter maps can be compared directly with ground based observations. We use magnetic field models derived from spacecraft measurements, and tailor the electron distributions to fit synchrotron observations. The gross features of data from both VLA and single-dish observations are fit by a longitudinally symmetric particle distribution. We suggest that higher order terms in the magnetic field, coupled with relativistic beaming effects of synchrotron radiation, are primarily responsible for the observed rotational asymmetry.

Introduction

Since the late 1950's, synchrotron radio emission from Jupiter, observed from the Earth, has been an important tool for understanding the magnetic field and relativistic electron population in the inner (1.2 to 3.5 Jovian radii) Jovian magnetosphere. Jovian synchrotron emission is reviewed in [*Carr et al.*, 1983] and elsewhere. High resolution radio maps of the synchrotron emission made with the VLA and other arrays have provided a wealth of information on the emission [e.g., *De Pater et al. 1997, Leblanc et al. 1997* and references therein]. Measurements from in situ spacecraft (Pioneers and Voyagers) and observations of Io's footprint [*Connerney et al.*, 1998] have greatly improved knowledge of the magnetic field, especially the higher order moments, but it has been difficult to characterize the relativistic electron population, which is determined by diffusion processes within the magnetosphere and by local sources and losses. Both synchrotron emission and scattering in the atmosphere contribute to the losses.

By comparing results from a computational model of the synchrotron radiation with ground based radio observations, we intend to improve the current knowledge of the relativistic electron population in the inner Jovian magnetosphere. Such modeling may also provide new information on high order moments of the field. In this paper we describe a computer model which calculates the synchrotron emission produced by a distribution of electrons trapped in a Jovian magnetic field, and present some initial results. With a simple, longitudinally symmetric electron distribution, the model reproduces the gross features of the observed emission. By comparing model results with data collected from single-dish and interferometric observations, we have begun to make inferences about Jupiter's magnetic field and the particles trapped within it.

Paper number 2000GL012087.
0094-8276/01/2000GL012087$05.00

The Model

Our model calculates the synchrotron emission produced by a set of particles in the Jovian magnetic field, as observed from a particular direction. In contrast to earlier models [e.g. *Dulk et al. 1999, De Pater 1981*], our model includes a true volume integral in 3-dimensional space and takes into account the relativistic beaming effects of synchrotron emission. Synchrotron emission is highly beamed in the instantaneous direction of motion, so the radiation from a spiralling electron is visible only as a brief pulse when its velocity vector is momentarily pointed towards the observer. To calculate the emission from a distribution of electrons, we sum up the pulses from all electrons whose pitch angle allows the velocity vector to align with the observer. Defining $\rho(E,\alpha)$ as the number of electrons per unit volume per unit energy per unit pitch angle at energy E and pitch angle α, the observed synchrotron emission can be described by its Stokes parameters [*Chang & Davis*, 1962; *Legg & Westfold*, 1968] as

$$I(f) = (CB/R^2)\int \rho(E,\alpha)F(x)dE \quad (1)$$

$$Q(f) = -(CBcos(2\chi)/R^2)\int \rho(E,\alpha)F_p(x)dE \quad (2)$$

$$U(f) = -(CBsin(2\chi)/R^2)\int \rho(E,\alpha)F_p(x)dE \quad (3)$$

$$V(f) = (CB/R^2)\int \rho(E,\alpha)(4/3)\ i\ cot\theta\ \times [2f/(3f_B sin\theta)]^{-1/2}\{(x)^{1/2}F_s(x) + [1+g(\theta)](x)^{-1/2}[F_p(x)-(1/2)F(x)]\}dE \quad (4)$$

where $x = f/f_c$, R is the observer's distance from Jupiter, $C = 3.73\times10^{-23}$ erg sec-1 gauss^{-1}, B is the local magnetic field, and E is the electron energy. α is the angle between the line of sight and the magnetic field, which is the pitch angle of observable electrons, as discussed below. Definition of the Stokes parameters Q and U requires a choice of basis vectors, here taken parallel to the Jovigraphic equator, so χ is the projected angle between the magnetic field and the Jovigraphic equator. F and F_p define the frequency dependence of synchrotron emission from a single electron [*Jackson*, 1975], and are defined in terms of modified Bessel functions as

$$F(x) = x\int_x^\infty K_{5/3}(\eta)d\eta \quad (5)$$

$$\text{and } F_p(x) = xK_{2/3}(x) \quad (6)$$

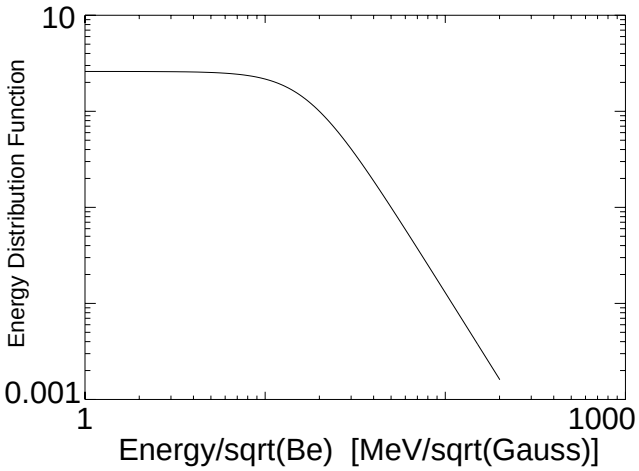

Figure 1. The energy distribution used for the examples shown in this paper.

Table 1. Example parameter set

L-Shell	n_1	n_2	A_L	
1.36-1.44	1.0	50	6.0	28.0
1.44-1.78	1.0	46	8.5	14.5
1.78-2.00	1.0	40	22.0	10.4
2.00-2.24	1.0	40	44.0	25.5
2.24-2.48	1.0	40	45.0	35.7
2.48-2.80	1.0	40	90.0	130.0
2.80-3.30	1.0	40	125.0	450.0
3.30-3.90	1.0	40	120.0	1160.0

Using these parameters (see Eq. 10), the model roughly fits the data. Parameters were chosen for each of 8 zones in L to match the resulting model images to VLA data taken in May of 1997. These parameter choices are used for all of the model results shown in this paper. Other parameter choices can result in similar qualitative agreement between model and data.

The characteristic frequency, f_c, is defined as

$$f_c = 3e/(4\pi m^3 c^4) B sin(\alpha) E^2. \quad (7)$$

To calculate the observed emission map, we integrate the local Stokes parameters over each line of sight at the frequency of observation.

In the formulation for I, Q, and U given by Eqs. 1 through 3 above, we have made the approximation that the opening angle of the synchrotron emission beam is small compared to the pitch-angle dependence of the electron distribution. The opening angle is inversely proportional to electron energy and is approximately 1.4° for 20 MeV electrons. Following [*Chang & Davis*, 1962], we account for the opening angle in calculating the total emission, but take the approximation that all of the radiation is emitted instantaneously at the time when the particle is moving directly towards the observer. Thus the pitch angle of all emitting particles is taken to be equal to the angle between the field and the line of sight. The circular polarization, V, is a result of the finite opening angle and the gradient of the pitch-angle distribution. Equation 4 is taken from [*Legg & Westfold*, 1968], along with the associated nomenclature. Typical observed circular polarization is $\sim 2\%$.

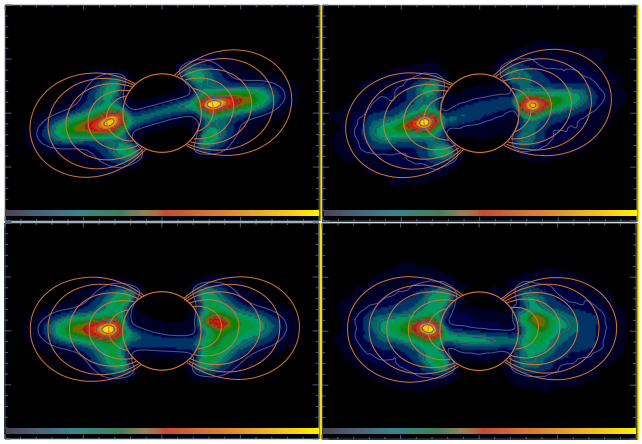

Figure 2. Comparison between VLA maps and the model (using parameters in Table 1) at 1400 MHz. The images represent model (left) and VLA (right) data for CML=120° (top) and 200° (bottom). Representative field lines taken from the VIP4 model are shown in the meridional plane for L-shells of 1.5, 2.0, 2.5, 3.0, and 3.5. Thermal emission from Jupiter has been subtracted. For each map, the color scale (shown at the bottom) is linearly normalized to the brightest pixel. Model maps are smoothed and averaged to approximate the spatial and temporal (longitudinal) resolution of the VLA observations. VLA data were taken in May, 1997.

In the computer model, we define the field and particle distributions on a 3-dimensional grid, and calculate the observed synchrotron emission by integrating Equations 1-4. The model inputs allow a choice of magnetic field model and electron density (as a function of pitch angle, energy and L-shell). Currently, we take the electron density to be

$$n_e(\alpha, L, B, E) = n_{e,\alpha}(\alpha, L, B)\; n_{e,E}(E, B) \quad (8)$$

where L is the L-shell, defined by

$$L = (M/B_e)^{1/3} \quad (9)$$

with B_e defined as the minimum magnetic field strength on the local field line and the magnetic dipole moment of Jupiter taken as $M = 4.218$ gauss-R_J^3. We further define

$$n_{e,\alpha}(\alpha, L, B) = A_L sin^{n1}(\alpha_{eq}) + B_L sin^{n2}(\alpha_{eq}) \quad (10)$$

and

$$n_{e,E}(E, B) = E_0/[E_0 + (\mathrm{E}/\mathrm{B}^{1/2})^{\epsilon+0.75}] \quad (11)$$

where A_L, B_L, n_1 and n_2 are functions of L, constant within each of an arbitrary number of zones, $\mathrm{E} = E/(1\ MeV)$, and $\mathrm{B} = B/(1\ Gauss)$. E_0 and ϵ are set at 5000 and 2.25 for all examples described in this paper, values chosen to roughly match the energy distribution from [*Divine & Garrett*, 1983] at $L = 2$ (Figure 1).

The atmospheric loss cone is approximated by modifying the electron distributions to remove all particles mirroring at $< 1\ R_J$ at any time during a longitudinal drift period. For purposes of this calculation, shell-splitting is ignored, with particles taken to drift on surfaces of constant L, defined as $(M/B_{eq})^{1/3}$. We have calculated drift shells more exactly by tracing particle motions adiabatically, and the shell-splitting is small compared to our 0.05 R_J resolution [*Wang*, 2000].

Taking as inputs A_L, B_L, n_1 and n_2 for each zone in L, the model produces as outputs a map of each of the I, Q, U,

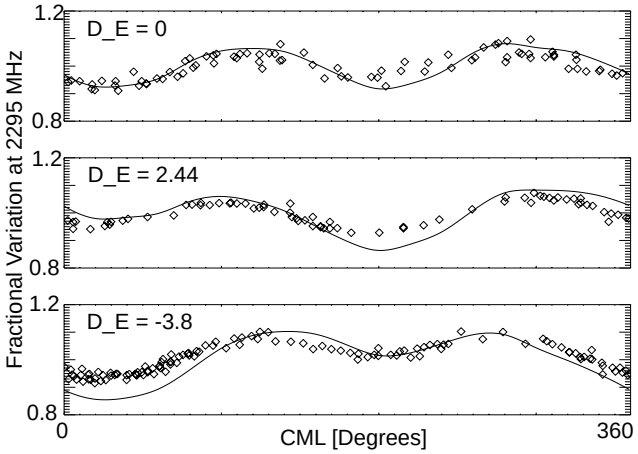

Figure 3. Observed and model beaming curves at 2295 MHz. Data were taken in 1997 (top panel), 1998 (middle panel), and 1994 (bottom panel), at times corresponding to different values of D_E , the Jovigraphic latitude of the sub-Earth point. The solid lines are model predictions (using the parameters in Table 1) for the corresponding D_E values of 0.0°, 2.44°, and -3.8°.

and V Stokes parameters, by numerically integrating Eqs. 1-4 at each point on a grid with spacing 0.05 R_J for the volume contained by $L < 4$. The Stokes parameters are then integrated along the line of sight (accounting for shadowing by Jupiter) to produce maps of the Stokes parameters with resolution 0.05 R_J. Model maps are made to correspond with different viewing geometries by rotating the magnetic field array prior to the calculation. For comparison with VLA data, maps from a range of CML's are averaged together (to account for time-averaging in the VLA data) and then smoothed with a 2-dimensional Gaussian beam whose size and shape are chosen to imitate the VLA resolution. For comparison with single-dish data, rotational averaging is not necessary, and the entire map is summed to produce a single total at each CML observed.

Discussion

The parameters $A_L(L)$, $B_L(L)$, $n_1(L)$ and $n_2(L)$ are chosen by comparing the resulting maps with observations. The parameters in Table 1 produce maps which qualitatively fit the observed VLA maps and beaming curves. The L-shell zones were chosen *a priori* to have physically plausible boundaries, and the parameters in each zone were then adjusted to produce reasonable maps. This was done iteratively, starting with an initial guess and successively modifying each of the $A_L(L)$ and $B_L(L)$ coefficients in an attempt to match the CML=0° VLA image. $n_2(L)$ was then adjusted (keeping $n_1(L)$ fixed at 1.0) to better match the East-West asymmetry [*Bolton et al.*, 2001], and the process repeated, with small adjustments to improve the beaming curve and the match at other CML's. We have produced qualitatively similar fits to the data using parameters which differ by ∼10% from those in Table 1, and also using the O6 [*Connerney*, 1993] instead of the VIP4 [*Connerney et al.*, 1998] magnetic field model. We have not fully explored variations of the energy distribution, but it is clear that a different energy distribution would require changes in the $A_L(L)$ and $B_L(L)$ coefficients.

Figure 2 shows modelled Stokes I emission at two different CML's, with the corresponding VLA images. The data were averaged over ±20° CML to improve the signal to noise ratio, so the same was done to the model maps, which have also been smoothed to approximate the elliptical shape of the effective VLA beam. Representative fieldlines are shown.

Figure 3 shows model beaming curves compared to single dish data at the same value of D_E, where the model Stokes I maps have been calculated at the appropriate frequency and totalled to produce a single total-power value at each CML. The model beaming curves look similar to the actual data, with no need for longitudinal asymmetry in the particle distributions. Similarly, Figure 4 shows that the East-West asymmetry in the equatorial lobes can be matched reasonably well to the data using longitudinally symmetric electron distributions. This result contradicts previous suggestions that a "hot spot" in Jupiter's radiation belts is needed to explain the asymmetry of the synchrotron emission [e.g. *De Pater* 1991]. By changing the pitch angle distribution of the equatorial particles, one can adjust the variation in the beaming curve and the East-West asymmetry in the equatorial lobes, so the parameters chosen (Table 1) reflect an attempt to fit the model to the May 1997 data. In May 1997 the Earth was in the Jovigraphic equatorial plane ($\mathrm{D}_E = 0$, top panel in Figure 3), but the same model parameters have also been used to simulate the emission that would be observed at other viewing angles, as shown in the lower panels of Figure 3.

The parameters in Table 1 were not adjusted to fit the polarization, but there is nonetheless rough agreement between the modelled polarization and the observational data. Summing over the entire map, our model produces average total linear polarization of 26% and average circular polarization of 5%, while the observed values are 20 to 25% and 2%.

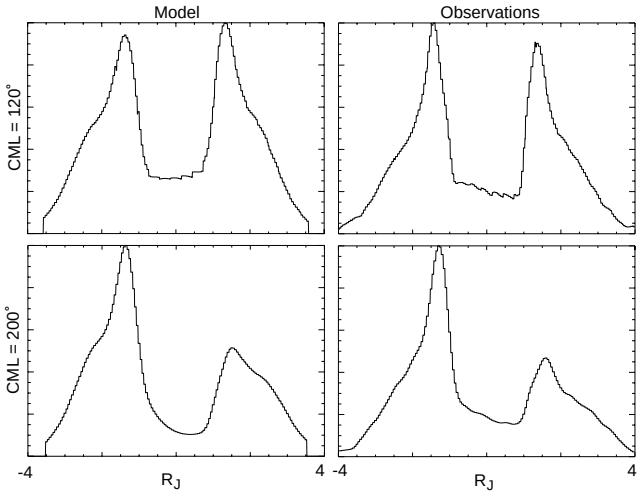

Figure 4. Comparison between model (left) and VLA observations (right) for a straight line cut along the magnetic equator. CML's of 120° (top) and 200° (bottom) are shown. In each panel, the plot is generated by extracting from the appropriate map (Figure 2) the brightness values along a straight line drawn through the magnetic equator (ie:; through the Jovigraphic equator for CML = 200° and at an angle of 9.85° for CML = 120°) and then normalizing to the peak brightness.

We plan improvements to the model in a number of areas, including better definition of the electron drift shells, more explicit calculation of the effects of synchrotron losses on the electron distributions, objective criteria for map comparisons, and more explicit derivation of particle distributions from first principles.

Acknowledgments. We appreciate the advice and assistance of Dr. Robert Sault and Dr. Kaiti Wang. This research was carried out at the Jet Propulsion Laboratory, California Institute of Technology, under a contract with the National Aeronautics and Space Administration.

References

Bolton, S.J., *et al.*, Divine Garrett Model and Jupiter's Synchrotron Radiation. *Geophys. Res. Lett.,* this issue.

Carr, T. D., M. D. Desch, and J. K. Alexander, Physics of the Jovian Magnetosphere, ed. A. J. Dessler, Cambridge University Press, 1983.

Chang, D.B., and L. Davis, Jr., Synchrotron radiation as the source of Jupiter's polarized decimeter radiation, *Astrophys. J., 126,* 567, 1962.

Connerney, J.E.P., Magnetic fields of the outer planets, *J. Geophys. Res., 98,* 18659-18679, 1993.

Connerney, J.E.P. *et al*, New models of Jupiter's magnetic field constrained by the Io flux tube footprint., *J. Geophys. Res., 103,* 11929-11939, 1998.

De Pater, I., A comparison of radio data and model calculations of Jupiter's synchrotron radiation, *J. Geophys. Res., 86,* 3397-3422, 1981.

De Pater, I., Radio images of Jupiter's synchrotron radiation at 6, 20, and 90 cm, *J. Geophys. Res., 102,* 794-805, 1991.

DePater, I., M. Schultz, and S. Brecht, Synchrotron evidence for Amalthea's influence on Jupiter's electron radiation belt, *J. Geophys. Res., 102,* 22043-22064, 1997.

Divine N., and H. B. Garrett, Charged particle distribution in Jupiter's magnetosphere:, *J. Geophys. Res., 88,* 6889-6903, 1983.

Dulk, G. A., Y. Leblanc, R.J. Sault, S.J. Bolton, J.H. Waite, and J.E.P. Connerney, Jupiter's magnetic field as revealed by the synchrotron radiation belts: I. Comparison of a 3-D reconstruction with models of the field, *Astron. Astrophys., 347,* 1029-1038, 1999.

Jackson, J. D. *Classical Electrodynamics, 2nd ed.,* John Wiley and Sons, 1975.

Leblanc, Y., R. Sault, and G. Dulk, Synthesis of magnetospheric radio emissions during and after the Jupiter/SL-9 collision, *Planetary Space Science, 45,* No.10, p.1213, 1997.

Legg, M.P.C., and K.C. Westfold, Elliptic Polarization of Synchrotron Radiation, *Astrophys. J., 154,* 499, 1968.

Wang. K., *private communication,* 2000.

S. Bolton, S. Gulkis, M. Klein and S. Levin, Jet Propulsion Laboratory, 4800 Oak Grove Drive, MS 169-506, Pasadena, CA 91109.
(e-mail: Scott.Bolton@jpl.nasa.gov; Samuel.Gulkis@jpl.nasa.gov; Michael.Klein@jpl.nasa.gov; Steven.Levin@jpl.nasa.gov)

B. Bhattacharya, R. Thorne, Department of Atmospheric Sciences, UCLA, Los Angeles, CA 90024.
(e-mail: bhattach@atmos.ucla.edu; rmt@atmos.ucla.edu)

(Received July 19, 2000; revised October 16, 2000;
accepted October 26, 2000.)